

Document downloaded from:

<http://hdl.handle.net/10251/104545>

This paper must be cited as:

Pasini Cabello, S.D.; Ochoa, N.; Takara, E.; Mollá, S.; Compañ Moreno, V. (2017). Influence of Pectin as a green polymer electrolyte on the transport properties of Chitosan-Pectin membranes. *Carbohydrate Polymers*. 157:1759-1768. doi:10.1016/j.carbpol.2016.11.061



The final publication is available at

<http://dx.doi.org/10.1016/j.carbpol.2016.11.061>

Copyright Elsevier

Additional Information

Manuscript Number:

Title: Influence of Pectin as a green polymer electrolyte on the transport properties of Chitosan-Pectin membranes

Article Type: Research Paper

Keywords: Biopolymeric membranes; polymer electrolyte membranes (PEM); methanol permeability; proton conductivity; differential scanning calorimetry (DSC); electrochemical techniques.

Corresponding Author: Prof. Vicente Compañ-Moreno, PhD

Corresponding Author's Institution: Universidad Politécnica de Valencia

First Author: Sergio D. Pasini Cabello, Dr.

Order of Authors: Sergio D. Pasini Cabello, Dr.; Nelio Ariel Ochoa, Dr.; Andres Takara; Sergio Mollá; Vicente Compañ-Moreno, PhD

Abstract: Novel composite membranes have been prepared from Chitosan (CH), Pectin (PEC) and their mixtures. The obtained samples were cross-linked and sulfonated before characterization. The results show that CH/PEC membranes display structural changes on the chemical and physical properties as a function of composition. DSC analysis reveals an endothermic peak due to the excision of the ionic pairs between carboxylic group and ammonium groups, which produces a strong change on physical properties such as methanol permeability and proton conductivity. The methanol permeability decreases with the amount of Pectin from $(4.24 \pm 0.04) \times 10^{-6}$ cm²/s for pure Chitosan membrane to $(1.51 \pm 0.03) \times 10^{-6}$ cm²/s for composite CH/PEC membranes when the amount of Pectin is 50% (v/v). The proton conductivities of the composite membranes follow a similar behavior. For a pure CH membrane the conductivity is 2.44×10^{-3} S/cm, decreasing with pectin content until the composition 50/50 (v/v), in which the conductivity is about one order of magnitude lower.

Suggested Reviewers: Luis F. del Castillo Dr.

Full Prof., Instituto de Materiales, Universidad Nacional Autónoma de México

lfelipe@unam.mx

Is a good specialist in the field of membranes characterization.

Santiago V. Luis Lafuente Dr.

Full Prof., Organic Chemistry, Universitat Jaume I. Castellón (Spain)
luiss@uji.es

He is the director of one of the best research groups in the preparation of Polymers and membranes in Spain.

Julio Guzman Dr.

Full Prof., Instituto de Polimeros, Consejo Superior de Investigaciones Científicas (CSIC). Madrid. Spain.

jguzman@ictp.csic.es

Is a good specialist in the syntesis and membranes preparation and its characterization.

Vicente Compañ
Departamento de Termodinámica Aplicada
Escuela Superior de Ingenieros Industriales
C/Camino de Vera s/n
46022. Valencia. Spain.
Phone: 34-96-3879328
Fax: 34-96-3877329
E-mail: vicommo@ter.upv.es

October 3, 2016

Dear Editor:

I submit to your consideration the publication in Carbohydrate Polymers the manuscript entitled
**“Influence of Pectin as a green polymer electrolyte on the transport properties of
Chitosan-Pectin membranes”**, written in collaboration with Dr. Sergio D. Pasini Cabello,
Dr. Noel Ariel Ochoa, Andres Takara and Dr. Sergio Mollá.

Thank you for your consideration.

Sincerely yours,

The authors.

Highlights

1. The effect of weight ratio of Chitosan (CH) to Pectin (PEC) is studied.
2. The methanol permeability of CH/PEC membranes decreases with the amount of Pectin.
3. Proton conductivities of CH/PEC membranes decrease until a ratio composition of 1:1.
4. DSC studies reveal excision of ionic pairs between carboxylic and ammonium groups.
5. Proton diffusion coefficients decrease one order of magnitude in CH/PEC membranes.

1 **Influence of Pectin as a green polymer electrolyte on the transport properties of**
2 **Chitosan-Pectin membranes.**

3

4 **S.D. Pasini Cabello^a, N.A. Ochoa^a, E.A. Takara^a, S. Mollá^b, V. Compañ^{b,*}.**

5 ^a: Instituto de Física Aplicada (INFAP). Universidad Nacional de San Luis CONICET.
6 Chacabuco 917 5700 San Luis, Argentina.

7 ^b: Departamento de Termodinámica Aplicada. Universidad Politécnica de Valencia. 46022-
8 Valencia, Spain.

9

10 (*) Corresponding author:

11 Vicente Compañ

12 Dpto. Termodinámica Aplicada

13 Universidad Politécnica de Valencia

14 46022-Valencia-Spain.

15 Tel.: +34963879328

16 Fax: +34963877924

17 e-mail: yicommo@ter.upv.es

18

19

20

21

22

23

24

25

26

27

28 **ABSTRACT**

29 Novel composite membranes have been prepared from Chitosan (CH), Pectin (PEC)
30 and their mixtures. The obtained samples were cross-linked and sulfonated before
31 characterization. The results show that CH/PEC membranes display structural changes
32 on the chemical and physical properties as a function of composition. DSC analysis
33 reveals an endothermic peak due to the excision of the ionic pairs between carboxylic
34 group and ammonium groups, which produces a strong change on physical properties
35 such as methanol permeability and proton conductivity. The methanol permeability
36 decreases with the amount of Pectin from $(4.24 \pm 0.04) \times 10^{-6}$ cm²/s for pure Chitosan
37 membrane to $(1.51 \pm 0.03) \times 10^{-6}$ cm²/s for composite CH/PEC membranes when the
38 amount of Pectin is 50% (v/v). The proton conductivities of the composite membranes
39 follow a similar behavior. For a pure CH membrane the conductivity is 2.44×10^{-3} S/cm,
40 decreasing with pectin content until the composition 50/50 (v/v), in which the
41 conductivity is about one order of magnitude lower.

42

43 **Keywords:** Biopolymeric membranes; polymer electrolyte membranes (PEM);
44 methanol permeability; proton conductivity; differential scanning calorimetry (DSC);
45 electrochemical techniques.

46

47

48

49

50

51

52

53 **1. Introduction**

54 The potential applications of biomaterials are numerous and involve different fields
55 such as fibers for the textile industry, medical products, cosmetics, bioimplant, delivery
56 of drugs, herbicides, fungicides, and so on. Biodegradability is nowadays considered to
57 be the most important factor for the introduction of new products. One of the most
58 promising approaches to overcome the safety and environmental problems is the use of
59 renewable resources for obtaining biodegradable polymers useful for various
60 applications in medical, pharmaceutical, agriculture, drug release, and packaging fields.
61 Pectin (PEC) is one of the naturally occurring polysaccharides that has become more
62 and more important over recent years, because this is a material with eco-friendly
63 properties primarily due to the renewability and sustainability of their sources. The
64 pectin has a low cost because of their abundance in nature (Cavallaro, Donato, Lazzara,
65 & Milioto, 2011; Pérez Espitia, Du, Avena-Bustillos, Ferreira Soares, & McHugh,
66 2014; Meneguín, Cury, & Evangelista, 2014). Pectin is a structural component of the
67 vegetal cell wall, typically isolated from plants of economic importance (citrus, sugar
68 beet, apple, etc.). It is composed of an anionic complex polysaccharide based on chains
69 of linear regions of (1 → 4)- α -D-galacturonosyl units and their methyl esters,
70 interrupted in places by (1 → 2)- α -L-rhamnopyranosyl units. Fractions of these
71 rhamnopyranosyl residues are branch points for neutral sugar side chains of (1 → 5)- α -
72 L-arabinofuranosyl or (1 → 4)- β -D-galactopyranosyl residues (Shols & Voragen, 1994;
73 Shols & Voragen, 1994). On the other hand, Chitosan (CH) is a linear copolysaccharide
74 β -(1 → 4)-2-amine-2-deoxy-d-glucose (GlcNac) and β -(1 → 4)-2-acetamine-2-deoxy-d-
75 glucose (GlcN). It is biodegradable, non-toxic, bio-compatible, and renewable (Croisier
76 & Jérôme, 2013; Sevel, İkinci, & Kas, 2000; Kaminski & Modrzejewska, 1997). Also, it
77 can be easily modified and has a noticeable ability to form many complexes with metal

78 ions and enzymes (Schmuhl, Krieg, & Keizer, 2001; Khor, 1997). In addition to its
79 many uses in food and agricultural applications, CH exhibits the ability to form films.
80 CH is obtained from Chitin, which is mainly extracted from crustacean exoskeletons
81 (Kurita, 2006; Muzzarelli, 1973). The solubility of polymers in aqueous acidic media
82 solutions has been used to distinguish chitin from CH. The word Chitosan has been used
83 for soluble polymers obtained from the deacetylation of chitin. Incomplete deacetylation
84 reaction allows for the random distribution of GlcNac and GlcN residues (Abdou, Nagy,
85 & Elsabee, 2008; Chang, Tsai, Lee, & Fu, 1997; Knaul, Kasaai, Bui, & Creber, 1998;
86 Tolaimatea et al., 2000). The degree of deacetylation (DDA) and molecular weights
87 (MW) determines some of the characteristics of CH, such as solubility,
88 biodegradability, aggregation properties and intrinsic ionic conductivity (Cho, Jang,
89 Park, & Ko, 2000; Kubota & Eguchi, 1997; Kristiansen, Vårum, & Grasdalen, 1998;
90 Liu, Adhikari, Guo, & Adhikari, 2013; Schatz, Pichot, Delair, Viton, & Domard, 2003).
91 DDA below 40–50% yields soluble polymers (Wang et al., 2008; Wang et al., 2006).
92 However membranes of Chitosan with DDA higher than 80% increases the crystallinity
93 improving their tensile strength and increasing the swelling but they may increase the
94 fragility and ionic permeability (Wan, Creber, Peppley, & Bui, 2003).

95 In the last years CH membranes has emerged as a new alternative to get membranes
96 with high ionic conductivity at low and moderate temperatures when the membrane is
97 completely or partially hydrated (Wan et al., 2003; Kordesch & Simader, 1996).
98 Chitosan membranes or hybrid Chitosan membranes can be used for an alkaline fuel
99 cell (AFC) where the ion OH^- carrier is required, because they are kinds of polar groups
100 on its backbone (hydroxyl and amino groups) that permit give to this kind of
101 membranes of hydrophilicity, which is the property more important for a fuel cell
102 (Krajewska, 2001; Zawodzinski et al., 1993). The use of this kind of membranes as

103 polymer electrolyte in a fuel cell has showed, operating at 60°C, a performance through
104 polarization curves (voltage-current density and power-current density) a current
105 density of 35mA/cm² in a PEMFC using hydrogen as feed into the anode and air as the
106 oxidant in the cathode (Wan et al., 2003). In previous studies (Wan et al., 2006),
107 alkaline chitosan-based composite membranes were prepared by incorporating KOH as
108 the functional ionic source The main problem is to hold the KOH permanently inside
109 the composite membrane avoiding the leaching of the bulk KOH into the polymeric
110 matrix. However preliminary studies into a real fuel cell system (FC) with membrane
111 electrode assembly of these composite membranes have shown at 60°C that a current
112 density of 35mA/cm² had been achieved using hydrogen as feed and air as the oxidant
113 (Wan et al., 2006).

114 Microbial fuel cell (MFC) is a promising technology for wastewater treatment as well as
115 means of energy recovery by microorganism. Various polymer membranes have been
116 developed to facilitate proton transfer between anode and cathode in MFCs (Seol et al.,
117 2012; Chae et al., 2008; Shaari & Kamarudin, 2015). Chitosan is a cheap and
118 environmental-friendly natural biopolymer, which is considered quite promising for its
119 use as a polymer electrolyte in MFCs (Smitha, Sridhar, & Khan, 2004). For these
120 reasons, the physical and chemical structure of CH must be modified to allow its use as
121 a viable polymer electrolyte membrane (Ma & Sajhai, 2013; Tripathi & Shadi, 2011;
122 Holder, Lee, Popuri, & Zhuang, 2016).

123 Blend, composites and multilayer films of PEC and CH with improved mechanical and
124 barrier properties have been previously described (De Yao et al., 1996; Hiorth, Tho, &
125 Arne, 2003; Hoagland & Parris, 1996; Sriamornsak & Puttipipatkachorn, 2004;
126 Milkova & Radeva, 2015; Pasini Cabello, Takara, Marchese, & Ochoa, 2015).
127 However, at the best of our knowledge there is not any report on CH/PEC films

128 functionalized with $-\text{SO}_3\text{H}$ groups that were characterized in order to reveal their
129 performance as a polymer electrolyte membrane. It is expected that the preparation of
130 composites membranes of CH/PEC in combination of acidic groups may give a
131 mechanical and chemical stability improved by the complexation due to the adsorption
132 of the different charges which originate Coulombic forces between the anions and
133 cations together with the functional groups of the CH and PEC. On the other hand, the
134 formation of ionic complex should produce a diminution of IEC and degree of swelling
135 which compact the polymer matrix. This leads to the formation of an ionic complex
136 with fewer carriers, providing a decreasing of conductivity when the ratio between CH
137 and PEC were 1:1.

138 In this paper we examine the effect of the weight ratio of CH to PEC following from the
139 chemical functionalization on the key transport properties such as methanol
140 permeability and membrane conductivity. Also, in order to reveal the structure of films
141 an approach based on FTIR spectroscopy and DSC analysis were performed. Water
142 uptake, mechanical properties and ion exchange capacity were also determined.

143

144 **2. Experimental**

145

146 **2.1 Materials**

147 Pectin from Citrus Fruits (CAS 9000-69- degree of methyl esterification, 6.7%, MW =
148 30 - 100 kg mol⁻¹) was purchased from Sigma-Aldrich (Denmark). A commercial
149 sample of CH powder of average viscometer molecular weight (890KDa), with
150 approximately 75% deacetylation, was supplied by Sigma-Aldrich. Glutaraldehyde
151 commercialized as 25% Grade II was purchased from Sigma-Aldrich (St. Louis, MO,
152 USA). Glycerol, acetone, H_3PO_4 , NaOH, NaCl, HCl, isopropanol and ethanol were

153 provided by BioPack (Campana, Argentina). All solutions were prepared with Milli-Q
154 water (resistivity > 1.8 mΩ cm). 4-formyl- 1,3-benzenedisulfonic acid disodium salt was
155 supplied by Aldrich.

156

157 **2.2 Preparation of the composite membrane**

158 The films made of Chitosan and Pectin and mixtures thereof were obtained by casting.
159 For this a polymer solution of CH and PEC with a mass fraction of 2% (w/v) was
160 prepared in distilled water containing Phosphoric Acid, 1% (v/v) at 40 °C. With
161 appropriate amounts of each solution, mixtures of different ratios were prepared in order
162 to obtain films named CH/PEC 100/0, 80/20, 60/40, 50/50, 40/60, 20/80 and 0/100,
163 respectively. Glycerol was added as a plasticizer at 0.5%. Film forming solutions were
164 cast in Petri dishes (14.5 cm internal diameter) and dried in an oven at 35°C for 48 h.
165 After that, the films were cross-linked, for this the films were immersing for 24 hours in
166 a room temperature bath consisting of 50 ml of acetone solution containing 5% (w/v)
167 glutaraldehyde (Sigma Aldrich) and 1% (w/v) HCl at 25°C. Finally, the films were
168 washed with ethanol and water. Film preparation was carried out in triplicate.

169

170 **2.3. Chemical functionalization**

171 In order to improve the ionic conductivity, sulfonic groups were added following the
172 same procedure reported elsewhere (Mollá & Compañ, 2011). Membranes were
173 immersed in a bath isopropanol/water (70/30 v/v) containing 0.04M 4-formyl- 1,3-
174 benzenedisulfonic acid disodium salt and 0,1M HCl for 2 h at 50°C. Then, several
175 washes of membranes were carried out with 0,3M HCl solution isopropanol/water
176 (70/30 v/v) in order to eliminate possible residual sodium ions. After that, the
177 membranes were dried at 50° C.

178

179 **2.4 Chemical stability of the membranes**

180

181 Vapor phase Fenton test has been developed to determine the membrane degradation as
182 an *ex situ* accelerated test method. Previously doped membranes with 2 ppm of aqueous
183 solution of FeSO₄ were vacuum dried and weighted. Then using a chamber similar to
184 reported by Delaney and Liu (Delaney & Liu, 2007), samples were suspended and
185 hydrogen peroxide added (3%) and the temperature was increased up to 80 degrees
186 centigrade using heating tape which was wrapped around the chamber. After test period,
187 the chamber was allowed to reach ambient temperature and the samples were removed,
188 dried and weighted again to determine weight loss.

189

190 **3. Membranes characterization**

191

192 **3.1. Ionic exchange capacity (IEC)**

193 The membranes were equilibrated in a solution of H₃PO₄ acid (2%) and GTA (5%)
194 overnight. The acidic membranes obtained were further washed several times with
195 distilled water and then equilibrated with a 1 M sodium chloride solution. The protons
196 delivered after the ion-exchange reaction $R-PO_4H_2^+ + Na^+ \rightarrow R-PO_4H_2Na + H^+$ were
197 titrated with a 0.01 M sodium hydroxide solution.

198

199 **3.2. Water uptake**

200 Water uptake of the CH/PEC membranes was measured by drying H⁺-form samples in a
201 vacuum and then weighed (W_s). For this the composite membranes were immersed in
202 distilled deionized water overnight. After that, the membranes were removed from
203 water, gently blotted with filter paper to remove excess surface water, and then weighed

204 again (W_w). This operation was repeated five times. Water uptake was calculated from
205 the difference between the weight of the composite wet and dry, by means of the
206 expression (1). The value of water uptake was averaged from three similar membranes
207 crosslinked at the same temperature and the results referred to the wet membrane are
208 given in Table 1.

209

$$210 \quad \% \text{ Water uptake} = \left(\frac{W_w - W_s}{W_w} \right) \cdot 100 \quad (1)$$

211

212 **3.3. Mechanical properties**

213 Tensile tests of the synthesized films were performed at room temperature using a
214 Comten Industries (Series 94 VC) device (Pinellas Park, Tampa FL, USA). Films were
215 cut into strips with a width of 1.1 cm and length of 4.0 cm. To ensure complete
216 relaxation of the polymeric structures and to standardize the experimental procedure,
217 film samples were stored in a humidity- and temperature-controlled chamber for 24 h at
218 25°C and 75% R.H. The polymeric strips were then fixed between upper and lower
219 clamps of the tensile tester and the tensile strength was determined at a constant traction
220 speed of 5 mm/min. The mechanical parameter data include the average values from
221 three samples of each film. The film thickness was measured using a Köfer micrometer
222 with a precision of $\pm 1 \mu\text{m}$.

223

224 **3.4. Differential scanning calorimetry (DSC)**

225 The DSC curves were obtained at 10 K/min under a nitrogen atmosphere (Melter
226 Toledo DSC 831). Two scans were performed with each sample, being the first from -
227 50°C to 80°C in order to remove the thermal history of the samples, and the second
228 from -50°C to 250°C.

229

230 **3.5. Methanol permeability**

231 In order to determine the methanol permeability coefficient through the composite
232 membranes, a typical 2-cell experimental set-up was used such as shown in a previous
233 paper (Mollá & Compañ, 2011), where the donor chamber was filled with 2M aqueous
234 solution of methanol, while the receptor chamber was filled with distilled water, both
235 chambers were kept under stirring and thermostated at 50°C.

236 As it is well described in another paper (Mollá & Compañ, 2015), the variation of
237 methanol concentration with time in the receiver reservoir (c_B) was determined by
238 means of a densimeter (DMA-4500M). A calibration curve of the density versus
239 methanol concentration is previously obtained. During those experiments, a small
240 sample of solution from the receiver compartment was taken at certain time intervals
241 and the density recorded. In order to avoid the volume of liquid in the receiver reservoir
242 (V_B) to change, the samples were recovered from the densimeter after each
243 measurement. Representing the normalized methanol concentration $(c_B L V_B)/(AC_A)$ vs.
244 time, the apparent permeability coefficient (P) of the methanol across the composite
245 membranes can be determined, by mean of the expression (2)

$$246 \quad C_B = \frac{P \cdot A}{L \cdot V_B} C_A \cdot t \quad (2)$$

247

248 **3.6. Membrane conductivity**

249 The conductivity of the composite membranes were measured by electrochemical
250 impedance spectroscopy (EIS) at different temperatures, in the frequency range $10^{-1} < f$
251 $< 10^6$ Hz. The experiments were performed with 0.1V amplitude, using a Novocontrol
252 broadband dielectric Spectrometer (Hundsangen, Germany) integrated by a SR 830
253 lock-in amplifier with an Alpha dielectric interface. The membranes were previously

254 equilibrated with deionized water (Milli-Q) and afterwards placed between two gold
255 electrodes in a parallel plate liquid sample cell (BDS 1308), Novocontrol) coupled to
256 the spectrometer. During the measurements the temperature was maintained below
257 isothermal conditions, controlled by a nitrogen jet QUATRO from Novocontrol with a
258 temperature error of ≈ 0.1 K during every single sweep in frequency. To obtain the
259 conductivity of the membranes four runs were carried out. The value of the conductivity
260 was obtained by taking the average of the four measurements and the uncertainty was
261 the SD from the mean value.

262

263 **4. Results and discussion**

264

265 **4.1. Water uptake and ionic exchange capacity**

266 In general the conductivity of acidic membranes depends on the water uptake and the
267 Ionic Exchange Capacity (IEC) of the membranes. The IEC represents the density of
268 sulfonic acid groups into the composite membrane. From the water uptake in the
269 channels of the composite hydrated the protons are present in the H_3O^+ form where the
270 hydrogen-bonded to water molecules is very strongly when the composite has higher
271 acid strength. Values of the water uptake and the IEC obtained for all the studied
272 membranes are given in Table 1. The results obtained for the water uptake show that
273 this parameter is very dependent on the amount of CH. For example, when the amount
274 of CH in the composite membrane is 20% and the amount of PEC is 80%, sample
275 (CH20/PEC80), the water uptake decreases about 80% from the value of pure Chitosan
276 membrane. However this decrease is about 60% for composites membranes of
277 CH50/PEC50, and for a pure Pectin membrane the water uptake is about 150% of the
278 previous, which means a 40% decrease from membranes of pure Chitosan. The ionic

279 exchange capacity (IEC) decreases from 0.37 meq/g for pure Chitosan (CH/PEC
 280 100/00) until 0.09 meq/g when the amount of Pectin is 50%. When the amount of Pectin
 281 increases until pure membrane 00/100, the IEC increases up to 0.36 meq/g. From the
 282 values given in Table 1 we can see that the IEC of pure membranes CH100/PEC00 and
 283 CH00/PEC100 are higher than composite membranes.

284

285 **Table 1.** Water uptake and ionic exchange capacity (IEC) for the CH/PEC membranes.

Membrane	Water uptake (%)	IEC (meq g ⁻¹)
CH100/PEC00	249±4	0.37±0.01
CH80/ PEC20	172±9	0.31±0.01
CH60/ PEC 40	141±7	0.26±0.1
CH50/ PEC50	91±5	0.09±0.01
CH40/ PEC 60	56±3	0.20±0.01
CH20/ PEC80	48±3	0.30±0.01
CH00/ PEC100	149±9	0.36±0.01

286

287 The change observed in the ionic exchange capacity of the composite membranes can
 288 be related with the formation of the ionic complex between the carboxyl groups of PEC
 289 and the ammonium groups of CH, since as we increase the amount of one of them, the
 290 amount of ionic groups also increase. This therefore increases the formation of
 291 interstitial clusters that will result in an increase of ionic carriers into the matrix of the
 292 composite membrane. On the contrary, when the ratio is 1:1, then the IEC decreases
 293 noticeably as ion carriers have been reduced due to the formation of a chemical
 294 structure wherein the polymer has been compacted and where the number of ionic
 295 groups has decreased probably due to the existing chain reaction between the two

296 polymers. As consequence of this, some structural changes related with the starting state
 297 are given respect to only PEC or CH. On the other hand, the decreasing of IEC in the
 298 composite membrane could be associated with the decreasing of water uptake which is
 299 related with the formation of the ionic complex between the carboxyl groups of Pectin
 300 and the ammonium groups of Chitosan.

301

302 4.2. Mechanical properties

303 Static tensile strength tests were carried out at room temperature following the
 304 experimental procedure described above. The experimental results are gathered in Table
 305 2.

306 **Table 2.** Membrane thickness, mechanical parameters, strain at yield point $\epsilon_y(\%)$,
 307 ultimate tensile strength σ_{ult} , and Young's modulus E measured at ambient temperature.
 308 In the last columns are given the methanol apparent permeabilities of CH/PEC
 309 composite membranes measured at 50°C.

%Chitosan	L(μm)	E (MPa)	ϵ_y (%)	σ_{ult} (MPa)	$P \times 10^6$ (cm^2/s)
100	395 \pm 2	7.2 \pm 0.4	4.9 \pm 0.6	28.7 \pm 1.1	4.24 \pm 0.04
80	277 \pm 2	7.4 \pm 0.5	7.7 \pm 0.8	29.3 \pm 0.7	3.26 \pm 0.06
60	219 \pm 2	7.6 \pm 0.3	13.8 \pm 2.2	30.3 \pm 1.5	2.29 \pm 0.02
50	222 \pm 2	5.6 \pm 0.2	6.3 \pm 1.3	34.6 \pm 1.0	1.51 \pm 0.02
40	182 \pm 2	5.5 \pm 0.1	4.4 \pm 0.7	21.7 \pm 1.8	2.33 \pm 0.06
20	193 \pm 2	5.3 \pm 0.8	1.8 \pm 0.8	19.5 \pm 1.9	3.10 \pm 0.05
0	257 \pm 2	3.9 \pm 0.8	10.2 \pm 1.9	18.6 \pm 1.7	3.90 \pm 0.04

310

311 From this Table we can see that the increase in Pectin produce changes in the
312 mechanical properties of the membranes. This could be related to the formation of the
313 ion pair. This interaction favors the increase in the yield strength ($\epsilon(\%)$), which can be
314 related to the electrostatic attraction possessing polymers that form the polymeric
315 matrix. This attraction tends to recompose the matrix to its original form and as the
316 amount of ionic bonds has been increased in the matrix then the polymer has greater
317 stretch ability than before fracture. The formation of an ionic pair produces an increase
318 in the ultimate tensile strength until the amount of Chitosan/Pectin is the same (1:1).
319 However the Young modulus increased while the amount of Chitosan decreased until
320 the ratio was 60% of Chitosan and 40% of Pectin. From this percentage the Young
321 modulus decreases by the incorporation of pectin into the chitosan matrix from 7.6MPa
322 for membranes of CH60/PEC40 until 3.9MPa for pure Pectin membranes. The same
323 behavior is observed for the yield strength, where this value increases from pure
324 Chitosan to composite membranes of CH60/PEC40, where the yield strength is about
325 300% higher than pure Chitosan membranes. From this ratio to CH80/PECc20 the yield
326 strength decreases about 600%. However, in the case of pure Pectin membranes the
327 yield strength is almost double the value of pure Chitosan membranes.

328 From these results we think that composite membranes of CH60/PEC40 have the best
329 mechanical properties to be used as sustainable membranes in green chemistry
330 applications. A comparison with Chitosan membranes, of high degree of deacetylation
331 and molecular weights (Wan et al., 2003) shows that our composite membranes have a
332 tensile strength and breaking elongation slightly smaller to this one however our
333 composite have a molecular weight of 2 or 3 times lower than the others. It could be due
334 to diminution of crystalline regions in our composite in comparison with the CH
335 membranes with high degree of deacetylation (DDA).

336 A comparison between CH/PEC and Sorbitol-Chitosan (S-CS) membranes and
337 phosphorylated-Chitosan membranes (CS-P) (Holder et al., 2016), shows that our
338 membranes have a tensile strength 100 times higher when the amount of pectin ranges
339 between 20-40%. On the other hand, CH/PEC membranes have a tensile strength 60%
340 smaller than CS-P with an elongation between 3 and 5 times smaller.

341

342 **4.3. Differential scanning calorimetry (DSC)**

343 DSC thermograms of sulfonated CH/PEC membranes with compositions 100/00, 60/40,
344 50/50, 40/60 and 00/100 at 10 K/min rate, under a nitrogen atmosphere, for 100 to
345 250°C range, using 0.5% glycerol (GLI) as plasticizer are shown in Figures 1a, 1b and
346 1c. CH/PEC 100/00 presents the typical Tg(I) and Tg(II) endothermic trials as it has
347 been reported when the second scan is performed (Mucha & Pawlak, 2005). Tg(I) at
348 118°C refers to water-plasticized chitosan macromolecules. Tg(II) at ~ 190°C attribute
349 to unplasticized chitosan macromolecules. As Mucha & Pawlak have pointed out,
350 referred to Tg (II), this event is a broad jump at 170-220°C, which can be recognized as
351 their Tg reflecting increase of molecular movement due to dissociation of hydrogen
352 bonds and starting of molecular chain scissions. However, those researchers have
353 performed their analysis with uncrosslinked chitosan. Other researchers (Neto et al.,
354 2005; Thacharodi & Panduranga, 1993; Jen & Wen, 2011) have addressed the
355 endothermic peak circa 170°C to the glutaraldehyde use as a crosslinking agent. They
356 informed that there were only endothermic events at 168°C using a single scan. The
357 authors suggested that glutaraldehyde can react with amine groups of chitosan. Thus,
358 water molecules will be bound to hydroxyl groups instead of amino groups, which are
359 less electronegative than hydroxyl ones. Therefore, the endothermic peak was shifted
360 from 133°C to 168°C for uncrosslinked and crosslinked chitosan, respectively. In our

361 study this explanations are complementary. The thermal behavior of pectin samples has
362 been previously described by Einhorn-Stoll et al. (Einhorn-Stoll, Kunzek, &
363 Dongowski, 2007; Einhorn-Stoll & Kunzek, 2009; Einhorn-Stoll & Kunzek, 2009).
364 These researchers mentioned that pectin thermal behavior depends on the chemical
365 composition and on state transitions, occurring during processing, as well as on the
366 interdependence of both factors. Some pectin samples showed an exothermic
367 degradation peak between 180-270°C. Also, an endothermic pre-peak appeared before
368 the degradation peak, corresponding to a conformational change that might be the
369 transformation from the more stable 4C_1 chair conformation of the galacturonan ring via
370 a boat conformation ${}^{1,4}B$ to the inverse 1C_4 chair conformation. Other researchers have
371 also observed that this conformational change has a higher free energy G (Marszalek et
372 al., 1999; Jarvis, 2002; Zhang & Marszalek, 2006; Haverkamp, Marshall, & Williams,
373 2007; Williams, Marshall, Anjukandi, & Haverkamp, 2007). These thermal events are
374 present in the DSC thermograms of CH/PEC 0/100. The pure pectin thermogram shows
375 an exothermic degradation peak at 234°C, and there is an endothermic pre-peak at
376 205°C. Also, at T=127°C another endothermic event similar to CH is observed related
377 to water-plasticized pectin macromolecules and the sulfonic groups are incorporated by
378 the functionalization of the reaction with 4-formyl-1-3-benzenedisulfonic acid.
379 From Figure 1 we can see that the thermograms of blend membranes are different from
380 those of pure polymers.

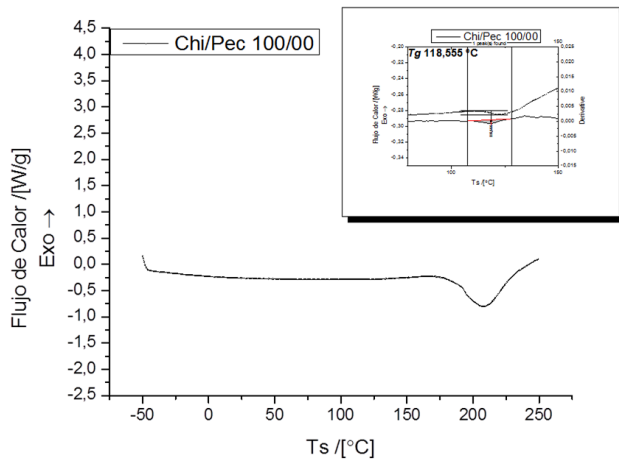
381

382

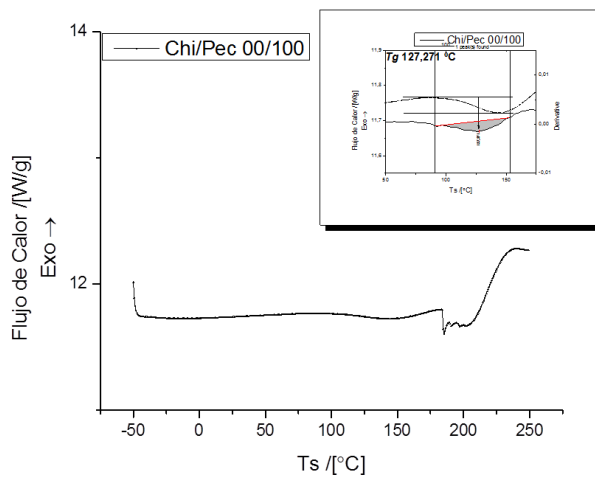
383

384

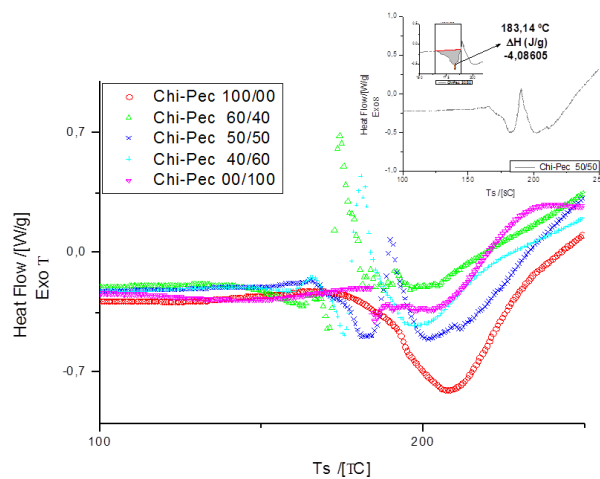
385



386



387



388

389 **Figure 1.** DSC thermograms of: a) CH100/PEC00, b) CH00/PEC100 and c) DSC of

390 CH/PEC blend membranes

391 Analysis of the DSC curve for the CH/PEC mixtures showed a pair of endothermic and
 392 exothermic peaks below 200°C. Blend membranes have an endothermic peak at 171.2,
 393 175.8 and 183.1°C for CH60/PEC40, CH40/PEC60 and CH50/PEC50, respectively, like
 394 are showed in Table 3. The detected endotherm is attributed to the evaporation of water
 395 tightly linked through polar interactions to ionic groups (Ribeiro, Silva, Ferreira, &
 396 Veiga, 2005) and can be assigned to the excision of an ion pair between the carboxylic
 397 group (-COOH) of the Pectin and the ammonium group (-NH₃⁺) of the Chitosan. All
 398 this is confirmed by the fact that the peak is shifted to the higher temperature as the
 399 composition of the membranes tends to be 1:1.

400

401 **Table 3.** Values of temperature and enthalpy corresponding to endothermic and
 402 exothermic peaks of blend membranes and pure polymers. In the last column we give
 403 the relative average molecular weight of membranes.

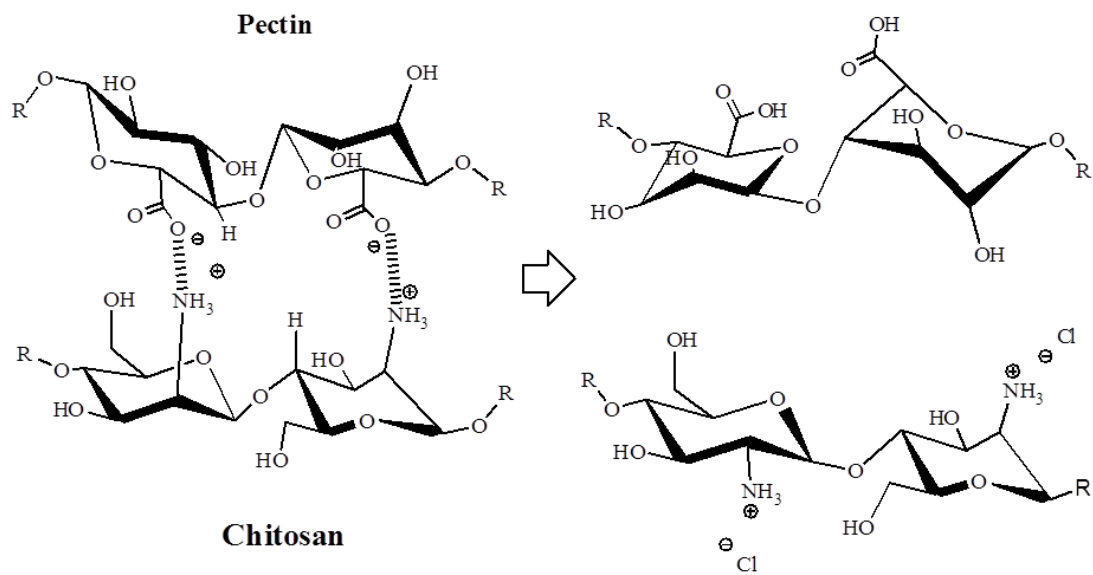
Membrane	Endothermic peak			Exothermic peaks			M _w
	T (°C)	ΔH (J/g)	ΔH (kJ/mol)	T (°C)	ΔH (J/g)	ΔH (kJ/mol)	
100-00	-	-		-	-		250000
60-40	171.2	-1.62	-285.01	174.3	5.2	915.2	176000
50-50	183.1	-4.09	-643.55	190.0	3.59	565.5	157500
40-60	175.8	-2.29	-317.74	180.9	7.36	1023.1	139000
00-100	-	-		-	-		650000

404

405

406

407



408
 409 **Figure 2.** Reaction to the excision of an ion pair between the carboxylic group (-
 410 COOH) of the Pectin and the amine group (-NH_3^+) of the Chitosan.
 411
 412 The representation of the reaction of the ionic complex ion between the two polymeric
 413 components of the CH/PEC membranes is shown in Figure 2, where the thermograms
 414 of blend membranes also shows the exothermic peaks corresponding to the subsequent
 415 relaxation of the molecular polymeric matrix. The peaks are centered at around 174.3,
 416 180.9 and 190.0°C for CH60/PEC40, CH40/PEC60 and CH50/PEC50, respectively,
 417 which could be assigned to the formation of an ionic pair between the carboxylate group
 418 (-COO^-) of pectin and the amine group -NH_3^+ of chitosan due to dehydration during
 419 the DSC scan. Similar results were found in CH/PEC, chitosan/alginate and
 420 chitosan/carboxycellulose blends (Ghaffari, Navaee, Oskoui, Bayati, & Rafiee-Tehrani,
 421 2007; Mayur, Rajashree, Jolly, & Vijay, 2007; Ostrowska-Czubenko & Gierszewska-
 422 Drużyńska, 2009; Rosca, Popa, Lisa, & Chitanu, 2005). From the area of the

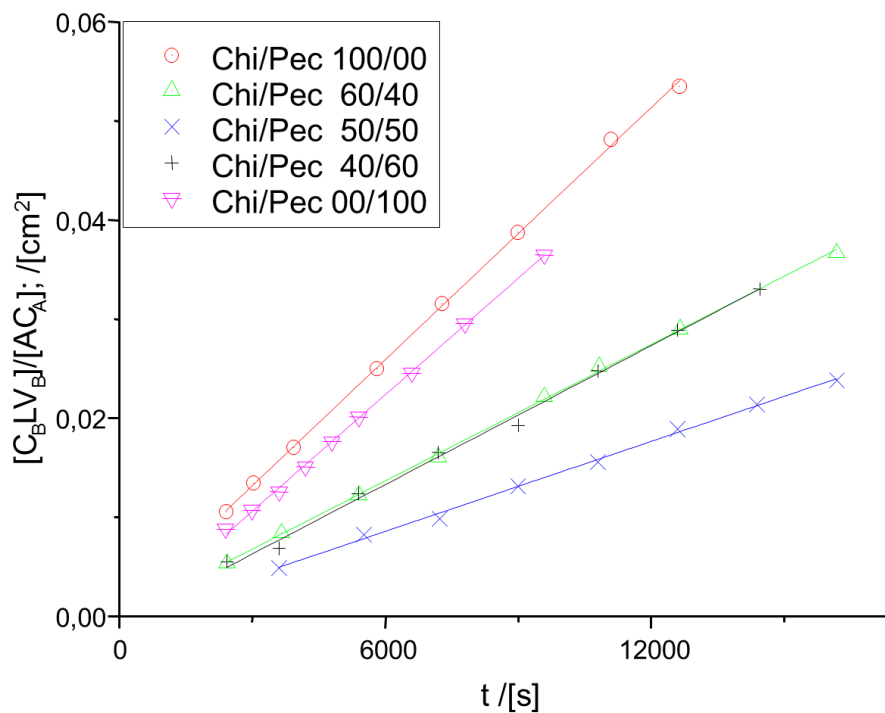
423 endothermic peaks we calculated the enthalpy of the process the excision of an ion pair
424 supposing that the relative average molecular weight of Chitosan and Pectin are 250000
425 and 65000, respectively. The values obtained are 285.0 kJ/mol (1.62 J/g), 317.7 kJ/mol
426 (2.29 J/g) and 643.5 kJ/mol (4.09 J/g) for CH60/PEC40, CH40/PEC60 and
427 CH50/PEC50, respectively. These results confirm the greater formation of complex ions
428 when membrane composition is tending to 1:1, point where it is necessary to give more
429 temperature and energy to break the complex. Finally in the thermograms we can see
430 that around 235°C of temperature the degradation of the Pectin begins to occur. Similar
431 results have been found by Gümüşoglu et al. (Gümüşoglu, Albayral, & Deligöz, 2011),
432 where the ionic interaction of the base polyelectrolyte complexes (PEC) membranes
433 formed by Chitosan and poly(acrylic acid (PAA) produce an enhancement of their
434 mechanical properties at least until 230°C.

435

436 **4.4. Methanol permeability**

437 The Methanol permeability has been measured analyzing the change of methanol
438 concentration in the receptor chamber. The temperature of the bath was fixed at 50°C
439 and donor chamber was filled with a 2M methanol solution. Samples of 500µl from
440 receptor chamber were taken within a period between 0 and around 4 hours. The
441 samples were analyzed by gas chromatography and their chromatograms compared with
442 the calibration curve, correlating the chromatograms peak areas with methanol
443 concentrations. The Figure 3 shows the function $(C_B \cdot L \cdot V_B / A \cdot C_A)$ versus time measured
444 at 50°C for CH/PEC membranes. Linear trends are obtained and the slopes estimated.
445 The values obtained from the slope of the plots permit us to obtain the apparent
446 methanol permeability of the membranes by means of eq.(2). In last column of Table 2
447 we can see the results obtained for the apparent permeabilities of CH/PEC membranes.

448 A close inspection of this Table shows that the permeability decreases when the
 449 concentration of Chitosan and Pectin in the membrane is 1:1, and increases when the
 450 membrane is pristine Chitosan and pristine Pectin, respectively. In the case of
 451 membranes where the amount of each polymer is different, such as CH60/PEC40 or
 452 CH40/PEC60, the apparent permeabilities are practically the same.



453
 454 **Figure 3.** Representation of $(C_B \cdot L \cdot V_B / A \cdot C_A)$ versus time of the CH/PEC composite
 455 membranes. The slope equates to the apparent methanol permeability.

456
 457 From the Table 2 we can observe that for CH100/PEC00 membranes the apparent
 458 methanol permeability is $(4.24 \pm 0.04) \times 10^{-6} \text{ cm}^2/\text{s}$, while for CH00/PEC100 this value is
 459 $(3.90 \pm 0.04) \times 10^{-6} \text{ cm}^2/\text{s}$. These values are quite similar to the values found for pristine
 460 Nafion® and Alginate90% /Carrageenan10% membranes where the apparent methanol
 461 permeabilities are about 2.2×10^{-6} and $4.0 \times 10^{-6} \text{ cm}^2/\text{s}$, respectively, but eight times
 462 higher than Alginate membranes (Pasini-Cabello et al., 2014). Low concentrations of

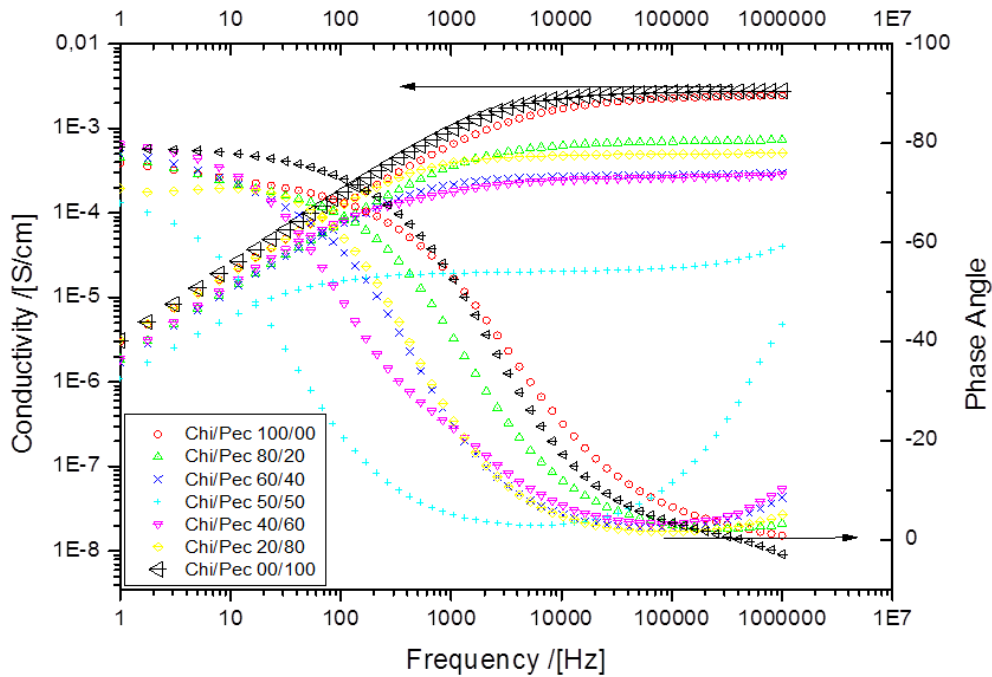
463 Pectin in the membranes have an effect similar to low concentrations of Chitosan in the
464 composed membranes. However, when the amount of Chitosan or Pectin increases in
465 the membrane the permeability decreases. This could be due to the reaction of the
466 formation of complex ions between the carboxyl groups of pectin and chitosan-
467 ammonium groups, producing a chemical structure more compact and stable due to the
468 possible reaction between the chains of both complexes, as shown in Figure 2. These
469 results also can produce a relative change of phase with significant changes in their
470 physical parameters, such methanol permeability, mechanical properties, swelling as
471 consequence of the compacting of its chemical structures in the formation of ionic
472 complex.

473

474 **4.5. Conductivity results**

475 Impedance spectroscopy measurements were carried out for CH/PEC membranes with
476 compositions 100/00, 80/20, 60/40, 50/50, 40/60, 20/80 and 00/100 at different
477 temperatures in order to obtain the conductivity and the diffusion coefficient of ionic
478 charge carriers. All the impedance measurements were done after hydration of the
479 composite membranes. From the dielectric measurements, the electrical conductivity σ
480 can be obtained from the imaginary part of the complex dielectric permittivity
481 ($\epsilon^* = \epsilon' - j\epsilon''$) where $\epsilon'' = \sigma / (\epsilon_0 \omega)$, being ϵ_0 the permittivity of vacuum and ω the angular
482 frequency of the applied electric field. The region where the slope of $\log \epsilon''$ versus $\log \omega$
483 is equal to -1 allows extrapolate to low frequencies and the intercept of this straight line
484 is the dc-conductivity (σ_{dc}). Alternatively, the data obtained can be analyzed in terms of
485 the Bode diagram (Compañ, Riande, Fernández-Carretero, Berezina, & Sytcheva, 2008;
486 Paddison, Kruer, & Maier, 2006). Typical plots of Bode diagram are shown in Figure 4.
487 This figure reveals that the real part of the conductivity increases with the frequency and

488 tends to a constant value when the phase angle, ϕ , reaches a maximum, for each
 489 temperature.



490

491 **Figure 4.** Bode diagram for the CH/PEC membranes obtained at 30°C of temperature.

492

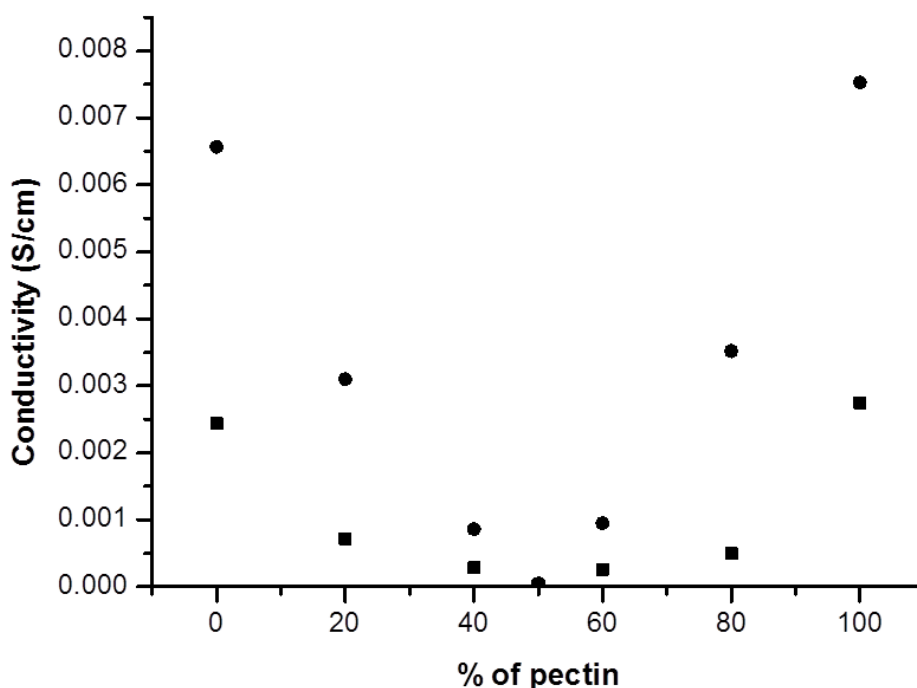
493 As it can be seen in Figure 4, all the samples, at 30°C of temperature, shown a plateau in
 494 the plot of the real part of the conductivity *vs* frequency in the region of moderate and
 495 high frequencies (10^3 to 10^6 Hz) coexisting with the peak of the phase angle or the
 496 tendency to the value zero. The value of the conductivity for which ϕ reaches a value
 497 practically equal to zero can be taken as the proton conductivity of the membrane.

498 Values of the conductivity for all the membranes of CH/PEC are given in Figure 5.

499

500

501



502

503 **Figure 5.** Conductivity of CH/PEC membranes with respect to the amount of pectin
 504 measured at 30°C (■) and 50°C (●), respectively.

505

506 As we can see, the conductivity for pristine Chitosan (CH100/PEC00) was 2.44×10^{-3}
 507 S/cm and 6.57×10^{-3} S/cm at 30 and 50°C respectively, decreasing when the amount of
 508 pectin increases, until the proportion of Chitosan and Pectin in the membrane is 1:1,
 509 where its conductivity is about two orders of magnitude smaller. These values are
 510 higher than estimated for membranes based on Chitosan crosslinked with
 511 glutaraldehyde (around 1.3×10^{-4} S/cm) (Majsztrik, Satterfield, Bocarsly, & Benziger,
 512 2007), but lower than membranes of Chitosan crosslinked in sulphuric acid (about
 513 1.83×10^{-2} S/cm) (Bass & Freger, 2008). On the other hand, our CH membranes have
 514 values of conductivity quite similar to the value found by Shirdast et al. 2.2×10^{-3} S/cm
 515 (Shirdast, Sharif, & Abdollahi, 2016), and lower than usually reported by others

516 researchers (Wan et al., 2006; Khiar, Puteh, & Arof, 2006). However our results are
517 more satisfactory due to our membranes have lower IEC (0.37 meq/g) than Shirdast et
518 al. which value was around 0.97 meq/g. The small differences found in conductivity can
519 be attributed to lower degree of deacetylation of Chitosan of this work (around 75%), in
520 comparison with those used by others (between 80 and 90%). On the other hand, our
521 membranes have values higher of IEC than obtained by others (Shirdast et al., 2016),
522 where CH and Sorbitol-Chitosan (S-CH) membranes had values of 0.24 and 0.30
523 meq/g, respectively. (Note that the abbreviation of Chitosan in other references (Holder
524 et al., 2016; Shirdast et al., 2016) is CS in place of CH used in our manuscript).

525 On the other hand, when the amount of Chitosan increases in the composite membrane
526 of CH00/PEC100, the conductivity has the same tendency. The conductivity for pristine
527 chitosan membranes varies from 2.75×10^{-3} S/cm at 30°C and 7.53×10^{-3} S/cm at 50°C to
528 the value of 5×10^{-5} S/cm for CH50/PEC50 membranes. The conductivities of our
529 membranes are one order of magnitude higher than the ionic conductivity found in
530 hydrated Chitosan membranes prepared from various degrees of deacetylation (DDA)
531 and different molecular weights from aqueous solutions of Chitosan and acid acetic
532 (Wan et al., 2003). This may be due to increased degree of crystallinity that Chitosan
533 DDA membranes possibly due to restricting the mobility of protons as a result of
534 increased stiffness of the polymer and tortuosity related to increased crystallinity.

535 A comparison between the conductivities of our composite membranes and those CH,
536 S-CH and phosphorylated-Chitosan (CH-P) membranes of other authors (Holder et al.,
537 2016) shown that our composites have an internal resistance comprised between 500
538 and 4500 Ω . These values are in the same order of magnitude than Chitosan (464 Ω),
539 Sorbitol-Chitosan (804 Ω) and Sorbitol-Phosphorylated-Chitosan membranes (2984
540 Ω) (Holder et al., 2016).

541 Electrochemical performance of CH, S-CH and CH-P membranes investigated in single
542 microbial fuel cells (MFCs) for bioelectricity generation have shown an excellent
543 behavior. The results of the performance and durability show that during bath cycle of
544 MFC operating with CH membrane, a maximum voltage of 152.6 mV was reached at
545 day 5 out of 7 days it took to reach cycle completion. The results are better when the
546 membrane used was S-CH, where this membrane was able to sustain a bath cycle for 12
547 days with maximum voltage of 464 mV with a power density of 94.59 mW/m². These
548 results are even better in the case of membranes of CH-P where the maximum voltage
549 was 504 mV and the maximum power density 130.03 mW/cm². When the membrane S-
550 CH-P was situated in the MFC system took 15 days to reach the maximum voltage of
551 294 mV (Holder et al., 2016). That means that this kind of membranes can sustain
552 themselves a lot of days until reach the end of cycle. These results allow us to think that
553 our membranes can also to be used as PEM in fuel cells such as PEMFC, DMFC or
554 MFCs.

555 The most important parameters to characterize and estimate the ionic transport in
556 polymers and membranes is the mobility associated to the total charge carrier
557 concentration. However, they are in general difficult to quantify and it is still at the
558 present time a matter of discussion in the scientific literature (Compañ et al., 2008). To
559 give an estimation of the diffusivity from the dielectric spectra we have considered the
560 model described previously based on the analysis of the dielectric spectra of the
561 electrode polarization where it is consider neglected the ion-ion interactions and
562 convection flux. Considering in first approximation that all the ionic capacity into the
563 membrane is involved in the distribution of ions that can move freely through the
564 membrane, the proton conductivity and ion diffusivity can be expressed according the

565 Einstein relation (Paddison et al., 2006), but a misprint in eq.(4) of this reference F was
566 written instead of F^2 , now the equation (3) is correctly stated as:

$$567 \quad \sigma = \frac{c_+ F^2 D_+}{RT} \quad (3)$$

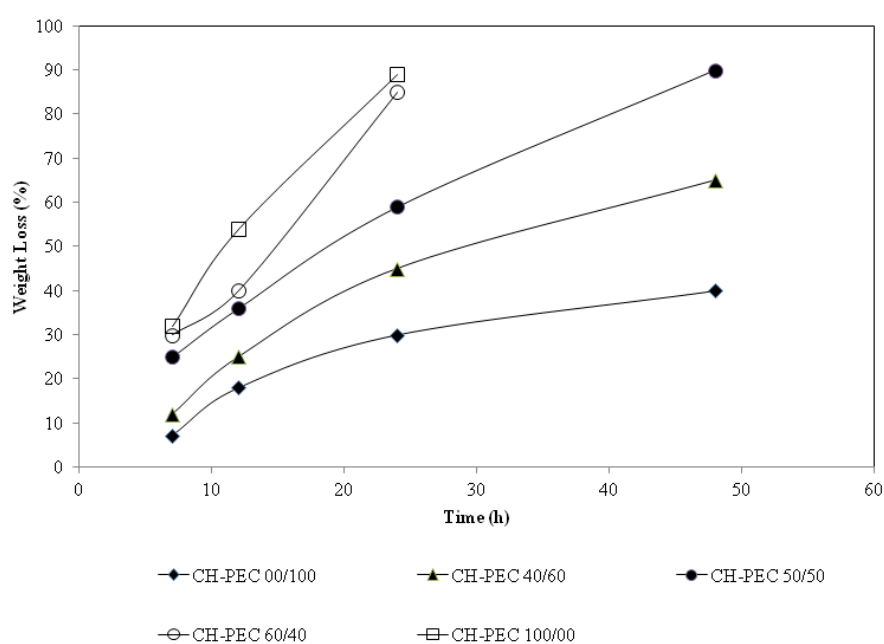
568 Where R is the universal gas constant, F the Faraday constant, T the absolute
569 temperature, c_+ the ionic exchange capacity and D_+ the proton diffusion coefficient. The
570 expression (3) permits us to obtain the diffusivity of the protons through the CH/PEC
571 membranes from the values of conductivity obtained from the Bode diagram and the
572 values measured for the ionic exchange capacity given in Table 1. The results found for
573 the diffusion coefficient shows that vary in proportion to the ratio (σ /IEC). The values
574 obtained at 30°C are 1.70×10^{-6} cm²/s and 2.0×10^{-6} cm²/s for pristine Chitosan and Pectin
575 membranes, where this value decreases for the composite membranes until the lowest
576 value of around 0.6×10^{-7} cm²/s is reached, corresponding to the CH50/PEC50
577 membranes. These values are quite close to that found in Nafion[®] 117 (Wan et al.,
578 2006; Khair et al., 2006), perfluorinated nanocomposite membranes modified by
579 polyaniline (Compañ et al., 2008) and bio-polymeric membranes of Alginate-
580 Carrageenan, but in such cases the membranes had less IEC and water uptake than this
581 one (Pasini-Cabello et al., 2014). As it is known the IEC and swelling of the membranes
582 will affect the ionic permeability through the membrane. In this sense the high degree of
583 swelling into the membrane will allow ions to move through the membrane increasing
584 its diffusivity in the swollen state. Such is shown in Table 1 the values of pristine
585 membranes have higher values of IEC and swelling than composite membranes. This
586 produces a significant increase in conductivity. This behavior could be due to the strong
587 interaction from the intramolecular hydrogen bonds between hydroxyl groups and
588 amine groups which are harder than intermolecular hydrogen interactions bonds
589 between polar groups and water.

590 The interest of CH is the tendency to acquire high hydrophilicity, very easy chemical
591 modification and good mechanical and thermal resistance. The CH with amino groups
592 present a polycationic character and form ionic cross links in presence of acidic groups
593 (Osugi, Dong, Hexig, & Inoue, 2007) producing polyelectrolytes complexes membranes
594 solving the dopant migration to give effective performance in DMFCs for prolonged
595 periods (Göktepe, Çelik, & Bozkurt, 2008). The main concern of this type of
596 membranes is the possible degradation, during cell operation conditions. In this way
597 some authors (Gümüşoğlu et al., 2011), have investigated the oxidative and hydrolytic
598 stability of Chitosan and poly(acrylic Acid) membranes found that can be suitable for
599 use in fuel cells such as DMFCs in which diluted methanol were used. In this way
600 hydrolytic and oxidative stability of the CH/PEC membranes were tested to investigate
601 the convenience for use as PEM in fuel cells. The hydrolytic stability of this type of
602 membranes was characterized controlling the time duration until membrane broken after
603 immersion in hot water. The results found for our membranes were around 125 hours
604 quite similar to PEC membranes which were more than 120 hours. These results show
605 that both kinds of membranes are suitable for fuel cells applications.

606 Several works have reported results from an *ex situ* vapor phase hydrogen peroxide test
607 (Delaney & Liu, 2007; Hommura, Kawahara, Shimohira, & Teraoka, 2008) and found
608 that gas phase hydrogen peroxide is very aggressive toward perfluorosulfonated (PFSA)
609 membrane, causes chain scissions in the backbone and in the side chain (Endoh, 2008).

610 In our membranes the *ex situ* vapor phase hydrogen peroxide test has allowed observe
611 the weight retention of our membranes as function of time, such as is shown in Figure 6.
612 A close inspection of this figure shows that the weight of each membrane decreases
613 gradually. On the other hand, we can observe that pure chitosan membranes (CH/PEC
614 100/00) are completely degraded after 24 h. This behavior has also been reported by

615 other researchers (Tian, Liu, Hu, & Zhao, 2004) and they have mentioned that this type
616 of change in the fundamental chitosan structure appears to be possible due to the role of
617 the amine group in the degradation of polysaccharides by hydrogen peroxide. The
618 glycoside bonds are more susceptible to split since there is an amine group adjacent to
619 the C₂ pyranose ring.



620

621 **Figure 6.** Chemical stability studies of CH/PEC membranes from Fenton test. In this
622 plot we observe the weight loss versus time using as Fenton's reagent in vapor phase
623 2ppm FFeSO₄ in 3wt% H₂O₂ at 80°C.

624

625 However, Pectin based membranes are more resistant to this test such as we can observe
626 from Figure 6 where an increase of amount of PEC produces a significant increase of
627 membranes durability. On the other hand, CH/PEC membranes allow fairly good
628 chemical stability as the sulfonation degree decreases, i.e the IEC decrease.

629 Therefore, our composite membranes with pectin and lower water uptake are expected
630 to take good chemical stability and durability than pristine CH membranes. As we have
631 seen in our composite membrane, adding Pectin to Chitosan or vice-versa the formation
632 of ionic complex produce a diminution of IEC and degree of swelling which compact
633 the polymer matrix, developing a loss of ionic groups until almost disappear as a
634 consequence of the ionic pair formation where the hydrophilic channels become more
635 compacted increasing the chemical stability and durability of the membranes.
636 Furthermore, we believe that CH/PEC membranes merits further investigation and
637 proportions of CH or PEC in the composite below than 40%, can be use as proton
638 exchange membranes for MFCs and DMFCs, using dilute methanol or ethanol as fuel.

639

640 **5. Conclusions**

641 To summarize, composite membranes of Chitosan and Pectin were obtained and
642 characterized. The pristine Chitosan and Pectin membranes showed higher proton
643 conductivities, IEC, water uptake and methanol permeability than composite
644 membranes of CH/PEC. This is due to the formation of an ionic complex, which
645 compacts the polymer matrix and therefore reducing the hydrophilicity of the channels.
646 When the ion pair between the carboxylic group (-COOH) of the Pectin and the amine
647 group (-NH₃⁺) of the Chitosan reacts, it is produced a diminution of content of amine
648 and carboxylic groups decreasing the hydroxyl groups and hence the hydrophilicity and
649 swelling of the membranes. When the content of the composite membrane is 50:50 wt,
650 the ionic strength fraction of the ions is practically the same, reducing around two
651 orders of magnitude its properties with respect to the ionic transport. Our results shown
652 that the methanol permeability is reduced, blocking off methanol molecules passing
653 through the membrane about three times more compared to pristine membranes. On the

654 other hand, the composite membranes with a content 50/50wt have ultimate tensile
655 strength σ_{ult} higher than the others possible due to the channels become more
656 compacted.

657 The *ex situ* vapor phase hydrogen peroxide test has allowed observe that the weight of
658 each membrane decreases gradually. Pristine chitosan membranes (CH/PEC 100/00) are
659 completely degraded after 24 h. This behavior can be possible due to the role of the
660 amine group in the degradation of polysaccharides by hydrogen peroxide. The glycoside
661 bonds are more susceptible to split since there is an amine group adjacent to the C₂
662 pyranose ring.

663 However, PEC based membranes are more resistant to Fenton's test where a increasing
664 of PEC produce a significant increase of membranes durability. On the other hand,
665 CH/PEC membranes allow fairly good chemical stability as the sulfonation degree
666 decreases, and by ender the IEC.

667 Then CH/PEC membranes merits further investigation and proportions of chitosan or
668 pectin in the composite below than 40%, can be rise to membranes presumably good
669 candidates for use as proton exchange membranes for MFCs and DMFCs, using dilute
670 methanol or ethanol as fuel. Additionally, the methodology presented in this work may
671 be extendable to other applications considering the influence of the amount of each
672 component into the composite membrane as consequence of the formation of the ionic
673 complex between the carboxyl groups of pectin and amine of chitosan, producing a
674 chemical structure more compact and stable due to the reaction between both groups.

675

676 **Acknowledgments**

677 This research has been supported by the ENE/2015-69203-R project, granted by the
678 Ministerio de Economía y Competitividad, Spain, and grants from ANPCyT,

679 Universidad Nacional de San Luis, CONICET, Argentina. Sergio David Pasini Cabello
680 thanks Erasmus Mundus Program for a EUROTANGO 2 fellowship at the Universidad
681 Politécnica de Valencia (UPV).

682

683 **References**

684 Cavallaro, G., Donato, D. I, Lazzara, G., & Milioto, S. (2011). Films of Halloysite
685 Nanotubes Sandwiched between Two Layers of Biopolymer: From the Morphology to
686 the Dielectric, Thermal, Transparency, and Wettability Properties. *The Journal of*
687 *Physical Chemistry C*, 115(42), 20491-20498.

688 Pérez Espitia, P. J., Du, W., Avena-Bustillos, R., Ferreira Soares, N., & McHugh, T. H.
689 (2014). Edible films from pectin: Physical-mechanical and antimicrobial properties - A
690 review. *Food Hydrocolloids*, 35, 287-296.

691 Meneguín, A. B., Cury, B. S. F., & Evangelista, R. C. (2014). Films from resistant
692 starch-pectin dispersions intended for colonic drug delivery. *Carbohydrate Polymers*,
693 99, 140-149.

694 Shols, H. A., & Voragen, A. G. J. (1994). Hairy (ramified) regions of pectin IV
695 Occurrence of pectin hairy regions in various plant-cell wall materials and their
696 degradability by rhamnogalacturonase. *Carbohydrate Research*, 256(1), 83-85.

697 Shols, H. A., & Voragen, A. G. J. (1994). Hairy (ramified) regions of pectin V. Isolation
698 and characterization of rhamnogalacturonan oligomers, liberated during degradation of
699 pectin hairy regions by rhamnogalacturonase. *Carbohydrate Research*, 256(1), 97-111.

700 Croisier, F., & Jérôme, C. (2013). Chitosan-based biomaterials for tissue engineering.
701 *European Polymer Journal*, 49(4), 780-792

702 Sevel, S., Ikinici, G., & Kas, S. (2000). Chitosan films and hydrogels of chlorhexidine
703 gluconate for oral mucosal delivery. *International Journal of Pharmaceutics*, 193(2),
704 197-203.

705 Kaminski, W., & Modrzejewska, Z. (1997). Equilibrium studies for the sorption of
706 metal ions onto chitosan. *Separation Science and Technology*, 32(16), 2659-2668.

707 Schmuhl, R., Krieg, H. M., & Keizer, K. (2001). Adsorption of Cu(II) and Cr(VI) ions
708 by chitosan: Kinetic and equilibrium studies. *Water SA*, 27(1), 1-7.

709 Khor, E. (1997). Methods for the treatment of collagenous tissues for bioprostheses.
710 *Biomaterials*, 18(2), 95-103.

711 Kurita, K. (2006). Chitin and chitosan: Functional biopolymers from marine
712 crustaceans. *Marine biotechnology*, 8(3), 203-226.

713 Muzzarelli, R. A. A. (1973). Chitin. In R. A. A. Muzzarelli (Ed.), *Natural Chelating*
714 *Polymers: Alginic acid, Chitin and Chitosan* (pp. 83-252). New York: Pergamon Press.

715 Abdou, E.S., Nagy, K. S. A., & Elsabee, M.Z. (2008). Extraction and characterization
716 of chitin and chitosan from local sources. *Bioresource Technology*, 99(5), 1359-1367.

717 Chang, K. L. B., Tsai, G., Lee, J., & Fu, W. R. (1997). Heterogeneous N-deacetylation
718 of chitin in alkaline solution. *Carbohydrate Research*, 303(3), 327-332.

719 Knaul, J. Z., Kasaai, M. R., Bui, V. T., & Creber, K. A. M. (1998). Characterization of
720 Deacetylated Chitosan and Chitosan Molecular Weight Review. *Canadian Journal of*
721 *Chemistry*, 76(11), 1699-1706.

722 Tolaimatea, A., Desbrieresb, J., Rhazia, M., Alaguic, A., Vincendond, A. M., &
723 Votterod, P. (2000). On the influence of deacetylation process on the physicochemical
724 characteristics of chitosan from squid chitin. *Polymer*, 41(7), 2463-2469.

725 Cho, Y. W., Jang, J., Park, C. R., & Ko, S. W. (2000). Preparation and solubility in acid
726 and water of partially deacetylated chitins. *Biomacromolecules*, 1(4), 609-614.

727 Kubota, N., & Eguchi, Y. (1997). Facile preparation of water-soluble N-acetylated
728 chitosan and molecular weight dependence of its water-solubility. *Polymer Journal*,
729 29(2), 123–127.

730 Kristiansen, A., Vårum, K. M., & Grasdalen, H. (1998). The interactions between
731 highly de-N-acetylated chitosans and lysozyme from chicken egg white studied by ¹H-
732 NMR spectroscopy. *European Journal of Biochemistry*, 251(1-2), 335-342.

733 Liu, H., Adhikari, R., Guo, Q., & Adhikari, B. (2013). Preparation and characterization
734 of glycerol plasticized (high-amylose) starch–chitosan films. *Journal of Food*
735 *Engineering*, 116(2), 588-597.

736 Schatz, C., Pichot, C., Delair, T., Viton, C., & Domard, A. (2003). Static light
737 scattering studies on chitosan solutions: From macromolecular chains to colloidal
738 dispersions. *Langmuir*, 19(23), 9896-9903.

739 Wang, W., Du, Y., Qiu, Y., Wang, X., Hu, Y., Yang, J., Cai, J., & Kennedy, J. F.
740 (2008). A new green technology for direct production of low molecular weight chitosan.
741 *Carbohydrate Polymers*, 74(1), 127-132.

742 Wang, Q. Z., Chen, X. G., Liu, N., Wang, S. X., Liu, C. S., Meng, X. H., & Liu, C. G.
743 (2006). Protonation constants of chitosan with different molecular weight and degree of
744 deacetylation. *Carbohydrate Polymers*, 65(2), 194-201.

745 Wan, Y., Creber, K. A. M., Peppley, B., & Bui, V. T. (2003). Ionic conductivity of
746 chitosan membranes. *Polymer*, 44(4), 1057-1065.

747 Kordesch, K., & Simader, G. (1996). Fuel Cell Systems. In *Fuel Cells and their*
748 *applications* (pp. 51-180). Weinheim, Germany: VCH.

749 Krajewska, B. (2001). Diffusional properties of chitosan hydrogel membranes, *Journal*
750 *of Chemical Technology and Biotechnology*, 76(6), 636-642.

751 Zawodzinski, T.A., Derouin, C., Radzinski, S., Sherman, R. J., Smith, V. T., Springer,
752 T. E., & Gottesfeld, S. (1993). Water uptake by and transport through Nafion 117
753 membranes. *Journal of The Electrochemical Society*, 140(4), 1041-1047.

754 Wan, Y., Creber, K. A. M., Peppley, B., & Bui, V. T. (2006). Chitosan-based electrolyte
755 composite membranes II. Mechanical properties and ionic conductivity. *Journal of*
756 *Membrane Science*, 284(1-2), 331-338.

757 Seol, J. H., Won J. H., Lee M. S., Yoon K. S., Hong Y. T., & Lee S. Y. (2012). A
758 proton conductive silicate-nanoencapsulated polyimide nonwoven as a novel porous
759 substrate for a reinforced sulfonated poly(arylene ether sulfone) composite membrane.
760 *Journal of Materials Chemistry* 22(4), 1634-1642.

761 Chae, K. J., Choi, M., Ajavi, F. F., Park, W., Chang, I. S., & Kim, I. S. (2008). Mass
762 transport through a proton exchange membrane (Nafion) in microbial fuel cells. *Energy*
763 *& Fuels*, 22(1), 169-176.

764 Shaari, N., & Kamarudin, S. K., (2015). Chitosan and alginate types of bio-membrane
765 in fuel cell application: An overview. *Journal of Power Sources*, 289, 71-80.

766 Smitha, B., Sridhar, S., & Khan, A. A. (2004). Polyelectrolytes complexes of Chitosan
767 and poly (acrylic acid) as proton exchange membranes for fuel cells. *Macromolecules*,
768 37(6), 2233-2239.

769 Ma, J., & Sajhai, I. (2013). Chitosan biopolymer for fuel cell applications. *Carbohydrate*
770 *Polymers*, 92(2), 955-975.

771 Tripathi, B. P, & Shadi, V. K. (2011). Organic-inorganic nanocomposite polymer
772 electrolyte membranes for fuel cell applications. *Progress in Polymer Science*, 36(7),
773 945-979.

774 Holder, S. L., Lee, C.-H., Popuri, S. R., & Zhuang, M.-X. (2016). Enhanced surface
775 functionality and microbial fuel cell performance of Chitosan membranes through
776 phosphorylation. *Carbohydrate Polymers*, 149, 251-262.

777 De Yao, K., Liu, J., Cheng, G. X., Lu, X. D., Tu, H. L., & Da Silva, J. A. L. (1996).
778 Swelling behavior of pectin/chitosan complex films. *Journal of Applied Polymer*
779 *Science*, 60(2), 279-283.

780 Hiorth, M., Tho, I., & Arne, S. S. (2003). The formation and permeability of drugs
781 across free pectin and chitosan films prepared by a spraying method. *European Journal*
782 *of Pharmaceutics and Biopharmaceutics*, 56(2), 175-181.

783 Hoagland, P. D., & Parris, N. (1996). Chitosan/pectin laminated films. *Journal of*
784 *Agricultural and Food Chemistry*, 44(7), 1915-1919.

785 Sriamornsak, P., & Puttipipatkachorn, S. (2004). Chitosan-pectin composite gel
786 spheres: Effect of some formulation variables on drug release. *Macromolecular*
787 *Symposia*, 216(1), 17-22.

788 Milkova, V., & Radeva, T. (2015). Influence of charge density and calcium salts on
789 stiffness of polysaccharides multilayer films. *Colloids and Surfaces A: Physicochemical*
790 *and Engineering Aspects*, 481, 13-19.

791 Pasini Cabello, S. D., Takara, E. A., Marchese, J., & Ochoa, N. A. (2015). Influence of
792 plasticizer in pectin films: Microstructural changes. *Materials Chemistry and Physics*,
793 162, 491-497.

794 Mollá, S., & Compañ, V. (2011). Performance of composite Nafion/PVA membranes
795 for direct methanol fuel cells. *Journal of Power Sources* 196(5), 2699-2708.

796 Delaney, W. E., & Liu, W. K. (2007). The Use of FTIR to Analyze Ex-situ and In-situ
797 Degradation of Perfluorinated Fuel Cell Ionomers. *ECS Transactions*, 11(1), 1093-104.

798 Mollá, S., & Compañ, V. (2015). Nanocomposite SPEEK-based membranes for Direct
799 Methanol Fuel Cells at intermediate temperatures. *Journal of Membrane Science*, 492,
800 123-136.

801 Mucha, M., & Pawlak, A. (2005). Thermal analysis of chitosan and its blends.
802 *Thermochimica Acta*, 427(1-2), 69-76.

803 Neto, C. G. T, Giacometti, J. A, Job, A. E., Ferreira, F. C, Fonseca, J. L. C., & Pereira,
804 M. R. (2005). Thermal Analysis of Chitosan Based Networks. *Carbohydrate Polymers*,
805 62(2), 97-103.

806 Thacharodi, D., Panduranga, R. K. (1993). Propranolol hydrochloride release behaviour
807 of crosslinked chitosan membranes. *Journal of Chemical Technology and*
808 *Biotechnology*, 58(2), 177-181.

809 Jen, M. Y., & Wen, Y. S. (2011). Preparation and characterization of chitosan hydrogel
810 membrane for the permeation of 5-Fluorouracil. *Materials Science and Engineering: C*,
811 31(5), 1002-1009.

812 Einhorn-Stoll, U., Kunzek, H., & Dongowski, G. (2007). Thermal analysis of
813 chemically and mechanically modified pectins. *Food Hydrocolloids*, 21(7), 1101-1112.

814 Einhorn-Stoll, U., & Kunzek, H. (2009). Thermoanalytical characterisation of
815 processing-dependent structural changes and state transitions of citrus pectin. *Food*
816 *Hydrocolloids*, 23(1), 40-52.

817 Einhorn-Stoll, U., & Kunzek, H. (2009). The influence of the storage conditions heat
818 and humidity on conformation, state transitions and degradation behaviour of dried
819 pectins. *Food Hydrocolloids*, 23(3), 856-866.

820 Marszalek, P. E., Pang, Y. P., Li, H. B., El Yazal, J., Oberhauser, A. F., & Fernandez,
821 J. M. (1999). Atomic levers control pyranose ring conformations. *Proceedings of the*
822 *National Academy of Sciences of the United States of America*, 96(14), 7894-7898.

823 Jarvis, M. C (2002). Biophysical properties of pectins. In G. B. Seymour, J. P. Knox
824 (Eds.), *Pectins and their manipulation* (pp. 99-130). Oxford: Blackwell Publishing.

825 Zhang, Q., & Marszalek, P. E. (2006). Solvent effects on the elasticity of
826 polysaccharide molecules in disordered and ordered states by single molecule force
827 spectroscopy. *Polymer*, 47(7), 2526-2532.

828 Haverkamp, R. G., Marshall, A. T., & Williams, M. A. K. (2007). Model for stretching
829 elastic biopolymers which exhibit conformational transformations. *Physical Review E*,
830 75(2), 021907.

831 Williams, M. A. K., Marshall, A. T., Anjukandi, P., & Haverkamp, R. P. (2007).
832 Investigation of the effects of fine structure on the nanomechanical properties of pectin.
833 *Physical Review E*, 76(2), 021927.

834 Ribeiro, A. J., Silva, C., Ferreira, D., & Veiga, F. (2005). Chitosan-reinforced alginate
835 microspheres obtained through the emulsification/internal gelation technique. *European*
836 *Journal of Pharmaceutical Sciences*, 25(1), 31-40.

837 Ghaffari, A., Navaee, K., Oskoui, M., Bayati, K., & Rafiee-Tehrani, M. (2007).
838 Preparation and characterization of free mixed-film of pectin/chitosan/Eudragit[®] RS
839 intended for sigmoidal drug delivery. *European Journal of Pharmaceutics and*
840 *Biopharmaceutics*, 67(1), 175-186.

841 Mayur, G. S., Rajashree, C. M., Jolly, M. S., & Vijay, B. S. (2007). Reversed chitosan–
842 alginate polyelectrolyte complex for stability improvement of alpha-amylase:
843 Optimization and physicochemical characterization. *European Journal of Pharmaceutics*
844 *and Biopharmaceutics*, 65(2), 215-232.

845 Ostrowska-Czubenko, J., & Gierszewska-Drużyńska, M. (2009). Effect of ionic
846 crosslinking on the water state in hydrogel chitosan membranes. *Carbohydrate*
847 *Polymers*, 77(3), 590-598.

848 Rosca, C., Popa, M. I., Lisa, G., & Chitanu, G. C. (2005). Interaction of chitosan with
849 natural or synthetic anionic polyelectrolytes. 1. The chitosan–carboxymethylcellulose
850 complex. *Carbohydrate Polymers*, 62(1), 35-41.

851 Gümüşoğlu, T., Albayral, G., & Deligöz, H. (2011). Investigation of salt addition and
852 acid treatment effects on the transport properties of ionically cross-linked
853 polyelectrolyte complex membranes based on chitosan and polyacrylic acid. *Journal of*
854 *Membrane Science*, 376(1-2), 25-34.

855 Pasini-Cabello, S. D., Mollá, S., Ochoa, N. A., Marchese, J., Gimenez, E., & Compañ,
856 V. (2014). New bio-polymeric membranes composed of alginate-carrageenan to be
857 applied as polymer electrolyte membranes for DMFC. *Journal of Power Sources*, 265,
858 345-355.

859 Compañ, V., Riande, E., Fernández-Carretero, F. J., Berezina, N. P., & Sytcheva, A. A.-
860 R. (2008). Influence of polyaniline intercalations on the conductivity and
861 permselectivity of perfluorinated cation-exchange membranes. *Journal of Membrane*
862 *Science*, 318(1-2), 255-263.

863 Paddison, S. J. Kruer, K. D., & Maier, J. (2006). About the choice of the protogenic
864 group in polymer electrolyte membranes: Ab initio modelling of sulfonic acid,
865 phosphonic acid, and imidazole functionalized alkanes. *Physical Chemistry Chemical*
866 *Physics*, 8(39), 4530-4542.

867 Majsztrik, P. W., Satterfield, M. B., Bocarsly, A. B., & Benziger, J. B. (2007). Water
868 sorption, desorption and transport in Nafion Membranes. *Journal of Membrane Science*,
869 301(1-2), 93-106.

870 Bass, M., & Freger, V. (2008). Hydration of Nafion and Dowex in liquid and vapor
871 environment: Schroeder's paradox and microstructure. *Polymer*, 49(2), 497-506.

872 Shirdast, A., Sharif, A., & Abdollahi, M. (2016). Effect of the incorporation of
873 sulfonated Chitosan/sulfonated graphene oxide on the proton conductivity of Chitosan
874 membranes. *Journal of Power Sources*, 306, 541-551.

875 Wan, Y., Creber, K. A. M., Peppley, B., & Bui, V. T. (2006). Chitosan-based electrolyte
876 composite membranes: II. Mechanical properties and ionic conductivity. *Journal of*
877 *Membrane Science*, 284(1-2), 331-338.

878 Khiar, A. S. A., Puteh, R., & Arof, A. K. (2006). Conductivity studies of a chitosan-
879 based polymer electrolyte. *Physica B: Condensed Matter*, 373(1), 23-27.

880 Osugi, N., Dong, T., Hexig, B., & Inoue, Y. (2007). Generation and characterization of
881 compositional gradient structure in the biodegradable chitosan/poly(ethylene oxide)
882 blend. *Journal of Applied Polymer Science*, 104(5), 2939-2946.

883 Göktepe, F., Çelik, S. Ü., & Bozkurt, A. (2008). Preparation and the proton conductivity
884 of chitosan/poly(vinyl phosphonic acid) complex polymer electrolytes. *Journal of Non-*
885 *Crystalline Solids*, 354(30), 3637-3642.

886 Hommura, S., Kawahara, K., Shimohira, T., & Teraoka, Y. (2008). Development of a
887 Method for Clarifying the Perfluorosulfonated Membrane Degradation Mechanism in a
888 Fuel Cell Environment, *Journal of The Electrochemical Society*, 155(1), A29-A33.

889 Endoh, E. (2008). Development of Highly Durable PFSA Membrane and MEA for
890 PEMFC Under High Temperature and Low Humidity Conditions, *ECS Transactions*,
891 16(2), 1229-1240.

892 Tian, F, Liu, Y., Hu, K., & Zhao, B. (2004). Study of the depolymerization behavior of
893 chitosan by hydrogen peroxide. *Carbohydrate Polymers*, 57(1), 31-37.